Journal of Thermal Analysis and Calorimetry (2023) 148:11683–11694
https://doi.org/10.1007/s10973-023-12507-4

Effect of PEG molecular mass and HEMA capping on the thermal, morphological, and hydrophilic properties of ısocyanate-terminated polyurethane acrylate films

Bilge Eren[1] · Esra Demir Karaçoban[1] · Beyhan Erdoğan[2] · Erdal Eren[3]

Received: 6 March 2023 / Accepted: 18 August 2023 / Published online: 8 September 2023

Abstract
The synthesis of isocyanate-terminated polyurethane prepolymers was carried out by reacting toluene diisocyanate (TDI) with an acrylic polyol, PEG-400, and PEG-1000, followed by capping the prepolymers with 2-hydroxyethyl methacrylate (HEMA) to produce polyurethane acrylates. The purpose of this study was to examine how different molecular masses of PEG and HEMA impact the thermal, morphological, and hydrophilic/hydrophobic properties of PUA films. The properties of the polyurethane acrylates were analyzed using various techniques, including DSC, FTIR, TGA, 1H NMR, SEM methods, and water contact angles and gloss tests. The results indicated that microphase separation morphology is prevalent within the PUA containing PEG-1000 and that the hydrophilicity of the PUA film is primarily influenced by the microphase separation behavior. The results revealed that the addition of PEG-400 improved the compatibility of hard and soft segments, leading to a shift toward phase mixing in the microphase separation behavior of PU acrylates. The microphase separation behavior was further studied using FTIR analysis of the C = O stretching vibration, with deconvolution performed using Origin software. The findings provide valuable insights into the structure–property relationships of PU acrylates, which can be utilized to optimize their performance for different applications.

Keywords Polyurethane acrylate (PUA) · İsocyanate-terminated · Microphase separation · 2-hydroxyethyl methacrylate (HEMA) · Phase mixing

Introduction

In recent years, acrylate functional urethane oligomers have gained widespread popularity as starting materials for various applications due to their excellent physical and mechanical properties [1, 2]. This has led to a growing interest in using polyurethane acrylates (PUAs) in coating applications. Many studies have demonstrated the significant properties of PUAs in various applications, and they have been found to have promising potential in a number of different fields, ranging from coatings to adhesives, and beyond. The versatility and unique properties of PUAs have made them an attractive option for many industries [3–15].

These studies highlight the impact of different factors on the properties of PUAs [3–8]. The degree of microphase separation has been shown to increase with the molecular mass of the soft segment [4]. The presence of acrylic acid and the use of different types of photoinitiators have been shown to impact the mechanical and chemical resistance of UV-cured coatings [5, 6]. The addition of reactive diluents and rigid diamine has also been found to influence the mechanical, chemical, and film properties of PUAs, as well as the microphase separation behavior and surface roughness [3, 7, 8]. These studies highlight the importance of understanding the relationships between various factors and the properties of PUAs in order to optimize their performance in different applications.

Xu et al. [9] show that waterborne PUA oligomers can be synthesized through an anionic self-emulsifying method using isophorone diisocyanate, polyether polyol, dimethylolpropionic acid, and hydroxyethylmethylacrylate as the

✉ Bilge Eren
bilge.eren@bilecik.edu.tr

[1] Department of Chemistry, Faculty of Science, Bilecik Seyh Edebali University, 11210 Bilecik, Turkey

[2] DYO Paint Factory, Ataturk Organize Sanayi, Bolgesi, TR-35620 Cigli Izmir, Turkey

[3] ErenChem YOSAB, 631. St. No: 13, İnegöl Bursa, Turkey

starting materials. This synthesis method provides a potential alternative to traditional solvent-based PUA oligomer synthesis, and the properties and potential applications of these waterborne PUA oligomers can be further studied. In the study conducted by Peruzzoa et al. [10], the behavior of PUA films was investigated in relation to the acrylic content. The authors found that the change in the properties of PUA films prepared by emulsion polymerization was nonlinear with increase in acrylic content. On the other hand, the change in properties of PUA films obtained through blending showed a gradual change based on the acrylic monomer content. In the study by Fu et al. [11], the Tg value of the hyperbranched polyurethane acrylate (PUA) hard coating was found to increase significantly in the presence of pentaerythritol tetra(3-mercaptopropionate). This was used to create protective films for the plastic caps of cell phones. The results demonstrate the potential of hyperbranched PUAs as a material for protective coatings in the electronics industry. Keramatinia et al. [12] found that the modification of hyperbranched polyamidoamine with glycidyl methacrylate led to a decrease in the Tg value of the hyperbranched polymers. However, the adhesion and flexibility of the polymer films improved. Kunwong et al. [13] reported that the synthesized hybrid organic-organic urethane acrylate oligomer showed good performance in terms of mechanical and film-forming properties. These results indicate that the hybrid organic-organic urethane acrylate oligomers can be promising materials for various coating applications. In their study, Yildiz et al. [14] found that the dual curable polyurethane methacrylate-based oligomers showed improved curing performance and mechanical properties in comparison with the single-cured oligomers. This indicated the potential of the dual curable oligomers in various adhesive applications. The study by Gite et al. [15] found that the properties of polyurethane coatings can be improved by increasing the NCO/OH ratio and hydroxyl content of acrylic polyols. The polyurethane coatings produced in the experiment showed good gloss, scratch resistance, and excellent adhesion.

The N–H group in polyurethane can form hydrogen bonds with either the C = O group of the hard domain or the ether C–O group of the soft domain. This bonding can be observed in infrared spectra where the broad carbonyl region has two contributions: free carbonyl groups that show a band around 1728 cm^{-1} and hydrogen-bonded carbonyl groups that show a band around 1704 cm^{-1} [16]. In PUAs, the bonded carbonyl groups can be divided into two bands, Band 1 and Band 2 [17]. Band 1 is the hydrogen bond between N–H and the carbonyl of the hard segment, while Band 2 is the hydrogen bond between N–H and the ether C-O of the soft segment. Band 1 hydrogen bonding results in higher microphase separation than Band 2 hydrogen bonding. The microphase separation behavior of PUAs can be monitored by analyzing the vibrations of the free and bonded carbonyl bands in the infrared spectra [17]. The microphase separation behavior in PUAs can be studied using the Hydrogen Bonding Index (HBI) which reflects the content of hydrogen bonds in the structure. A higher HBI value indicates a higher content of hydrogen bonds and thus a lower interaction between the soft and hard domains. An increase in hydrogen bonding leads to an increase in the HBI values [16].

The properties of PUAs are dependent on their microphase separation behavior. The microphase separation morphology within PUAs is affected by the incompatibility between the hard and soft segments. The aim of the study was to examine the influence of the chemical structure of polyurethane acrylates (PUA) on microphase separation within PUA. To achieve this goal, the study synthesized NCO-terminated polyurethane oligomers by combining toluene diisocyanate (TDI) with PEG-400, PEG-1000, and the acrylic polyol to form prepolymers, which were then capped with 2-hydroxyethyl methacrylate (HEMA). The chemical and physical properties of PUAs were characterized using DSC, FTIR, TGA, 1H NMR, SEM methods, and water contact angles and gloss tests. To understand the microphase separation of PUAs, the FTIR was used to investigate the degree of hydrogen bonding between the hard and soft domains. The deconvolution of overlapped free and bonded carbonyl vibration bands of PUA was performed using Origin software to understand the microphase separation behavior.

Experimental

Materials and instrumentation

Polyethylene glycol 400 (PEG-400, 98%), polyethylene glycol 1000 (PEG-1000, 99%), 2-hydroxyethyl methacrylate (HEMA, 99%), dibutyltin dilaurate (DBTDL, 95%), toluene diisocyanate (TDI), and acetone (99.8%) were purchased from Aldrich. The acrylic polyol was purchased from Allnex. The acrylic polyol had a solid content of approximately 61% and a hydroxyl value of approximately 4.2% (based on non-volatiles).

The ^{1}H NMR spectrum was obtained by the Varian Oxford NMR-300 spectrometer in DMSO (DMSO-d_6). The thermal stability of the PUAs was tested by an EXSTAR SII TGA/DTA 7200 model thermal analyzer. The studied temperature range was adjusted from 30 to 1000 °C by heating at 10 °C min^{-1}. The glass transition temperature (T_g) of the PUAs was obtained by a Perkin Elmer DSC 6000 under N_2 atmosphere in the temperature range of -50 °C to 150 °C C by heating at 10 °C min^{-1}. Fourier transform infrared (FTIR) spectra were obtained by a PerkinElmer Spectrum-100 FTIR spectrometer. The gloss of the PUA films was tested with a Byk Micro TRI

Gloss at an angle of 20°, 60°, and 85°. The contact angle was measured by a Attension Theta Lite, Hamilton Syringe 1001 TPLT. The surface of the PUA films was studied with a ZEISS Supra 40 VP model scanning electron microscopy (SEM).

Table 1 Composition of the prepared PUA samples

PU sample label	Soft Segment	Molar ratio of acrylic polyol/HEMA
$PUA_{4\text{-}2/0}$	PEG-400	2/0
$PUA_{4\text{-}1/1}$	PEG-400	1/1
$PUA_{4\text{-}0/2}$	PEG-400	0/2
$PUA_{10\text{-}2/0}$	PEG-1000	2/0
$PUA_{10\text{-}1/1}$	PEG-1000	1/1
$PUA_{10\text{-}0/2}$	PEG-1000	0/2

Synthesis of polyurethane acrylate

The composition of PUAs is shown in Table 1. The representative reaction used in this study is shown in Scheme 1. The PUAs were synthesized by the acetone process, where a diol (PEG), DBTDL (0.3%) and acetone (60 mass%) were mixed in a flask and then TDI was added dropwise over a period of one hour. The mixture was then heated at 40 °C for 2 h under a reflux condenser. After this, HEMA was added dropwise and heated again for 2 h to obtain the isocyanate ended urethane acrylate oligomer. Lastly, the acrylic polyol was gradually added and the reaction was stirred for 3 h until the isocyanate group was completely reacted, as determined by the IR spectra. The PUAs are designated as $PUA_{x\text{-}y/z}$, where x shows the molecular mass of PEG and y/z indicates the mol ratio of acrylic polyol/HEMA. For example, $PUA_{4\text{-}1/2}$ shows the PUA with PEG-400 having acrylic polyol/HEMA ratio of 1/2.

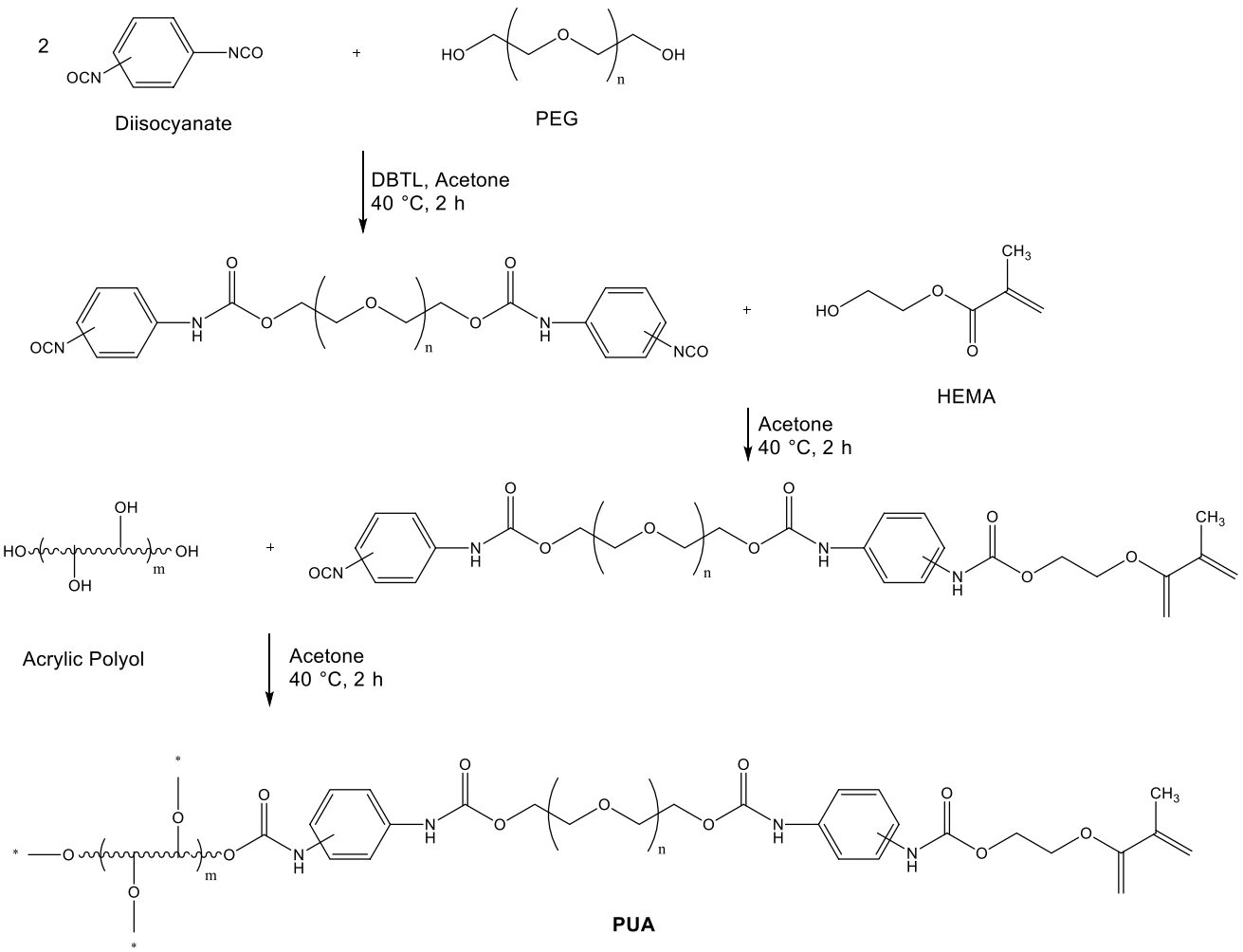

Scheme 1 Synthetic procedure of PUA oligomer for the acrylic polyol/HEMA ratio of 1/1

Results and discussion

Structural characterization of PUA

The ^{1}H-NMR spectrum of $PUA_{4\text{-}1/1}$ dissolved in DMSO-d6 is presented in Fig. 1. It was chosen as the exclusive representative example for this study because of the highly restricted solubility observed in other PUAs. The presence of NH protons at the expected frequency in the spectrum confirms the formation of the polyurethane functional group. The presence of NH protons at 9.68, 9.03, and 8.90 ppm indicates the success of the reaction between TDI, PEG and the acrylic polyol, and HEMA, resulting in the synthesis of the desired polyurethane acrylate oligomers. The spectrum also shows signals at 7.53 ppm and 7.14 ppm, corresponding to the aromatic protons in the TDI monomer, while the vinyl protons of the HEMA group give rise to signals at 6.04 ppm and 5.69 ppm. The protons of ethoxy groups at PEG and acrylic polyol units generate signals between 4.66 and 4.15 ppm, while the aliphatic protons (CH_3, CH_2, and CH) of the acrylic polyol units produce signals between 2.49 and 0.80 ppm. These spectral signals are consistent with the previously published results [17].

The FTIR spectrum of $PUA_{4\text{-}2/0}$ is shown in Fig. 2. The peaks at 2923 and 2871 cm^{-1} in the spectrum are associated with the asymmetric and symmetric stretching vibrations of CH_2, respectively, and indicate the presence of aliphatic chains in the PUAs. This suggests the presence of acrylic polyol units in the PUAs. The band at 1180–1071 cm^{-1} in the FTIR spectrum is attributed to the C-O stretching vibration of the ether functional group in PEG-400. This band is characteristic of the carbon–oxygen bond stretching in ether functional groups and is commonly seen in spectra of compounds containing ether groups. The lack of the NCO (isocyanate) absorption band at 2270 cm^{-1} in the FTIR spectrum indicates that the TDI has reacted completely with the acrylic polyol and PEG-400 to form polyurethane. This suggests that no residual isocyanates are present in the polyurethane oligomers. The spectrum of PUA exhibits common characteristic bands, such as N–H stretching at 3301 cm^{-1}, C = O stretching at 1722 cm^{-1}, CH bending at 1451 cm^{-1}, NH bending at 1534 cm^{-1}, and C–O stretching of ether at 1223 cm^{-1}. These bands are associated with specific vibrations of the molecular bonds in the PUA molecule [17–20].

The spectrum of $PUA_{4\text{-}1/1}$ shows typical vibration bands of polyurethanes, including H-bonded NH stretching at 3300 cm^{-1}, asymmetric CH_2 stretching at 2923 cm^{-1}, C = O stretching at 1717 cm^{-1}, C–O–H bending at

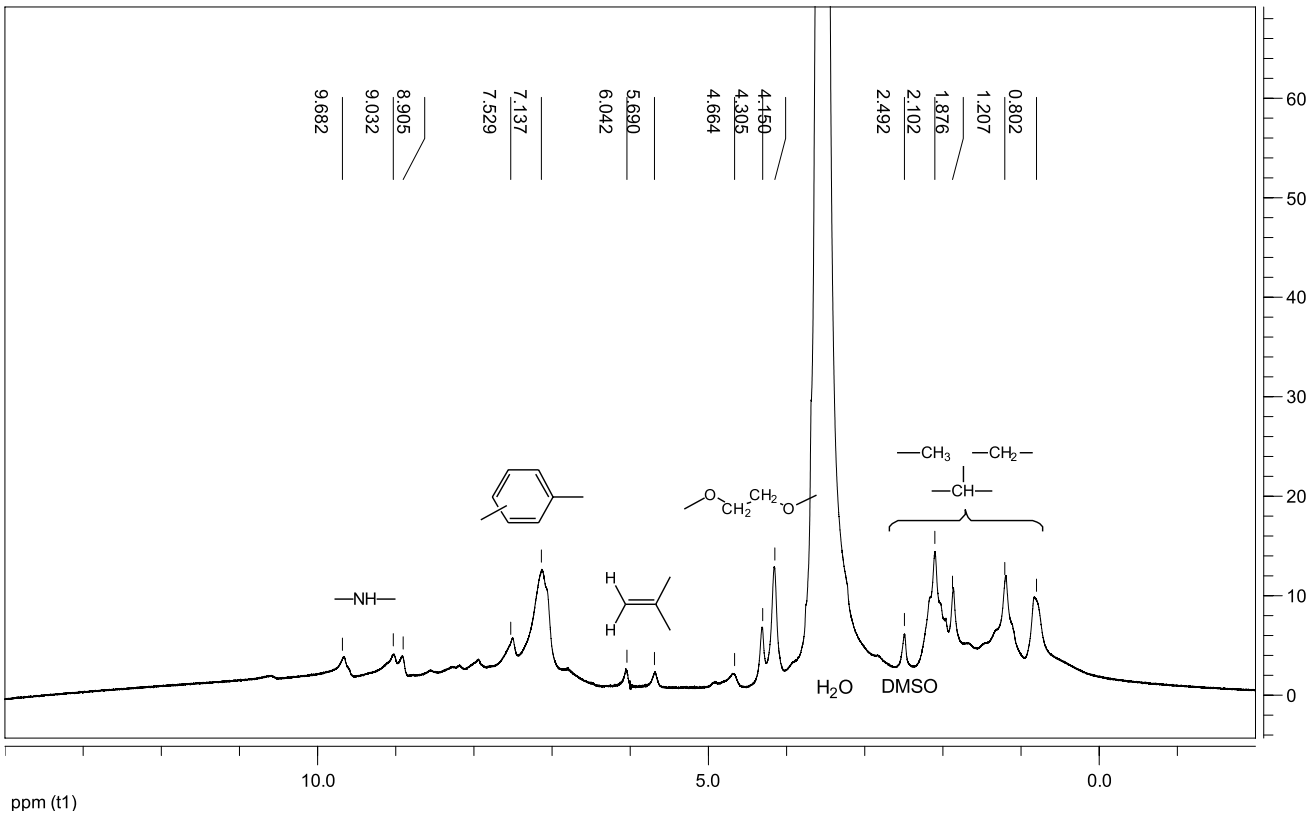

Fig. 1 ^{1}H-NMR Spectrum of $PUA_{4\text{-}1/1}$ in DMSO-d_6

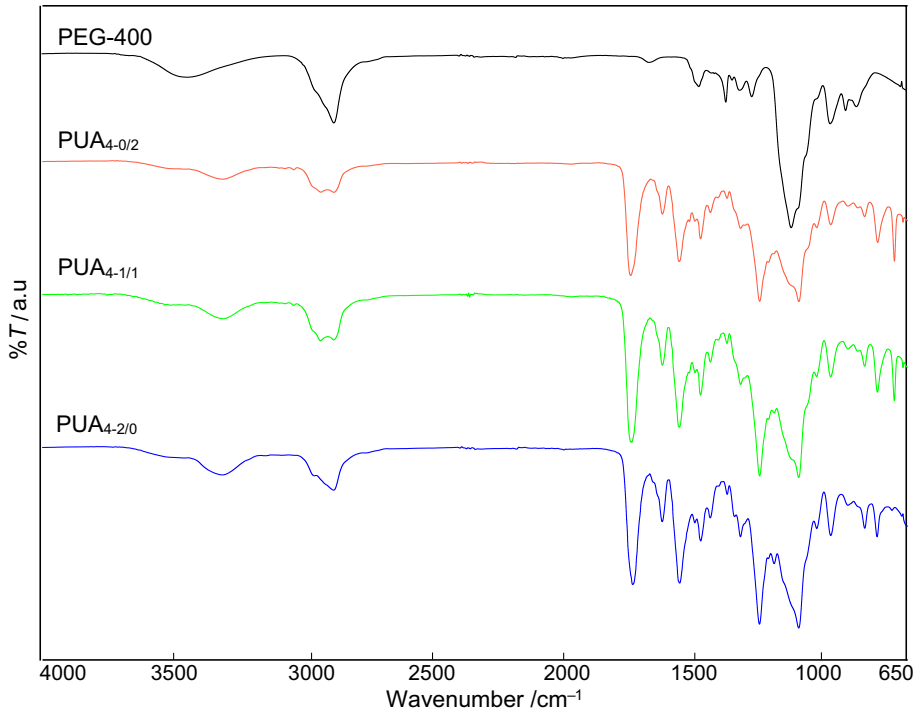

Fig. 2 IR spectra of PUA samples with PEG-400 showing characteristic stretching bands

1452 cm^{-1}, and out-of-plane OH deformation at 1349 cm^{-1} (Fig. 2). These bands indicate specific vibrations of the molecular bonds in $PUA_{4\text{-}1/1}$ and help to identify the material as a polyurethane. The band at 1600 cm^{-1} in the spectrum is attributed to the C = C stretching of HEMA. The bands at 1188 cm^{-1} and 1105 cm^{-1} are related to the vibration of ether C–O of PEG-400 and acrylic polyol, respectively. These specific vibrations of the molecular bonds help to identify the materials present in the spectrum [17–20].

The $PUA_{4\text{-}0/2}$ spectrum showed a characteristic band at 1714 cm^{-1}, which indicates the C = O stretching of urethane groups. The NH deformation band was observed at 1533 cm^{-1}, and the CH2 bending vibration band was seen at 1451 cm^{-1}. The presence of ether C-O groups in $PUA_{4\text{-}0/2}$ with PEG-400 was confirmed by the C–O stretching vibration bands at 1223 cm^{-1} and 1071 cm^{-1}. These bands are specific to the molecular structure of $PUA_{4\text{-}0/2}$ and provide important information about the material. The absence of free amine bands at 3467 cm^{-1} in the spectrum indicates that the amine groups have formed hydrogen bonds with the C = O in urethane [21]. This information helps to understand the molecular structure of the material. Additionally, the disappearance of the broad band at 3550–3300 cm^{-1}, which is associated with the OH stretching vibration of PEG, confirms that the OH groups on PEG and the acrylic polyol have undergone complete conversion to the urethane structure. These bands provide important information about the molecular structure and reactivity of the materials present in the spectrum (Fig. 3).

PUA exhibits microphase separation due to the thermodynamic incompatibility between its hard and soft segments, which impacts its microstructure and performance. The vibrational bands of the urethane structure's free and hydrogen-bonded C = O groups were examined to study this behavior. The hydrogen-bonded carbonyl and free carbonyl bands appeared at 1712–1714 cm^{-1} and 1718–1731 cm^{-1}, respectively, providing crucial information about PUA's microphase separation behavior and its effect on the material's properties. Distinguishing between the hydrogen-bonded and free C = O groups can be difficult because the hydrogen-bonded and free carbonyl bands overlap in the spectrum. The Origin software was used to deconvolute the two overlapped free and bonded carbonyl vibration bands, enabling the precise identification of the hydrogen-bonded and free C = O groups. This provides more accurate information about the material's molecular structure and reactivity, as shown in the supplementary file, Fig. S1-S6.

Two parameters, the hydrogen bonding index (HBI) and the degree of phase separation (DPS), can be used to detect the microphase separation of a material. Equations (1) and (2) can calculate these parameters, respectively. The HBI gives information about the strength of the hydrogen bonds in the material, while the DPS provides information about the degree of separation between the hard and soft segments. Both parameters are crucial indicators of the material's microphase separation behavior and can be used to evaluate its performance and predict its properties.

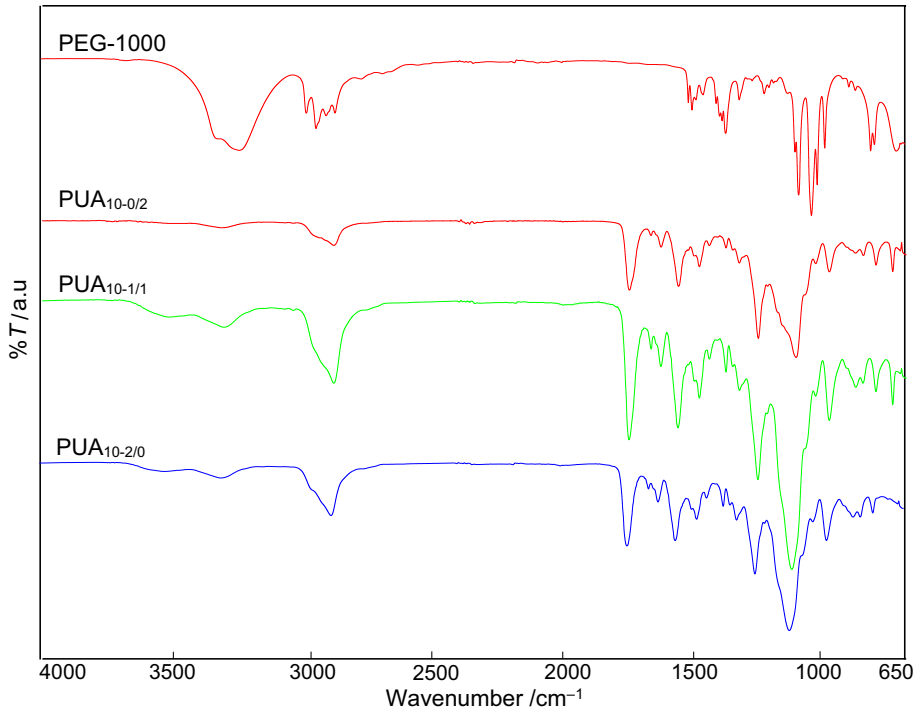

Fig. 3 IR spectra of PUA samples with PEG-1000 showing characteristic stretching bands

Table 2 Gauissian fitting data for the carbonyl peak area in the FTIR spectra of PUAs

Sample	Free urea	Bonded urethane	Free urethane	HBI	DPS
$PUA_{4\text{-}2/0}$	1694	1712	1730	1.80	0.64
Area	0.89	1.98	1.10		
$PUA_{4\text{-}1/1}$	1695	1713	1730	2.20	0.69
Area	1.73	4.31	1.96		
$PUA_{4\text{-}0/2}$	1699	1714	1731	3.78	0.79
Area	2.60	4.12	1.09		
$PUA_{10\text{-}2/0}$	–	1713	1729	2.93	0.75
Area	–	0.79	0.27		
$PUA_{10\text{-}1/1}$	1688	1712	1729	1.27	0.56
Area	0.20	2.17	1.71		
$PUA_{10\text{-}0/2}$	–	1714	1728	2.63	0.72
Area	–	3.15	1.20		

$$\mathrm{HBI} = \frac{S_{\mathrm{bonded}}}{S_{\mathrm{free}}} \tag{1}$$

$$\mathrm{DPS} = \frac{\mathrm{HBI}}{\mathrm{HBI} + 1} \tag{2}$$

In the equation, S_{bonded} represents the area of the hydrogen-bonded carbonyl band, while S_{free} represents the area of the free carbonyl band [21]. The HBI is calculated as the ratio of S_{bonded} to the sum of S_{bonded} and S_{free}. The calculated HBI values for PUAs can be found in Table 2. These values provide information about the strength of the hydrogen bonds in the material and help to understand the microphase separation behavior of PUA.

The HBI values obtained for $PUA_{4\text{-}2/0}$, $PUA_{4\text{-}1/1}$, and $PUA_{4\text{-}0/2}$ were 1.80, 2.20, and 3.78, respectively (Table 2). A higher HBI value signifies a greater degree of hydrogen bonding between the carbonyl and urethane NH groups, which increases the interaction between the urethane NH groups and the ether C-O groups in the soft segments, leading to increased microphase separation. The $PUA_{4\text{-}0/2}$ sample exhibited the highest HBI value of 3.78, indicating the strongest hydrogen bonding among the PUAs. This finding can be attributed to the high content of HEMA in $PUA_{4\text{-}0/2}$. The results suggest that the chemical structure of PUA significantly influences the hydrogen bonding and microphase separation in PUA.

The HBI values for $PUA_{4\text{-}1/1}$, $PUA_{4\text{-}0/2}$, $PUA_{10\text{-}1/1}$, and $PUA_{10\text{-}0/2}$ were found to be 2.20, 3.78, 1.27, and 2.63, respectively. The results indicate that an increase in the content of HEMA in the polymer chain leads to a corresponding increase in the HBI. This effect is attributed to the stronger hydrogen bonding interactions that arise between the hard domains contributed by HEMA, leading to higher microphase separation while the length of the soft segment remains constant. These findings offer valuable insights into the relationship between the HEMA content and the microstructural characteristics of PUA polymers. The observed increased degree of microphase separation is primarily due to the rise in hydrogen bonding interactions between the carbonyl and urethane NH groups, which leads to stronger segregation of the hard and soft segments and, consequently,

higher phase separation [21]. Additionally, the incorporation of HEMA, a hydrophilic monomer, into the polymer chain further reduces the compatibility between the soft and hard segments, resulting in an increase in the degree of microphase separation.

DSC studies

The behavior of microphase separation in the polymers was studied using DSC measurements, and the obtained results were confined to a temperature range below 150 °C due to the degradation observed in certain formulations beyond this temperature. This degradation is evident from the DTG curves presented in Sect. "TGA Studies".

The DSC curves showed one glass transition, indicating the presence of at least one glassy amorphous phase (Figs. 4, 5). The T_g values of PUA were found to range from -38.03 to 26.26 °C. The *T*g value for $PUA_{10\text{-}2/0}$ was − 32.60 °C, while the T_g value for $PUA_{4\text{-}2/0}$ was 26.26 °C (Table 3). $PUA_{10\text{-}2/0}$ had a lower T_g value compared to $PUA_{4\text{-}2/0}$, which suggests that it has a more flexible and rubbery nature due to the higher compatibility between the soft and hard segments, which is attributed to the similarities in polarity between PEG-400 and TDI.

As shown in Table 3, the T_g values of $PUA_{4\text{-}2/0}$ and $PUA_{4\text{-}0/2}$ were calculated as 26.26 °C and − 18.76 °C, respectively. This is consistent with the increase in HBI values from 1.80 for $PUA_{4\text{-}2/0}$ to 3.78 for $PUA_{4\text{-}0/2}$ (Table 2). As previously mentioned in Sect. "Structural characterization of PUA", the $PUA_{4\text{-}2/0}$ with lower HBI values and more phase mixing had a lower ratio of bonded to nonbonded urethane carbonyl [18, 21, 23].

The introduction of HEMA into PUA decreased its T_g value by causing microphase separation. This was due to hydrogen bonding forming between the hard and soft segments, reducing the mobility of PUA chains. DSC results showed that the microphase separation was smallest in films prepared with $PUA_{4\text{-}2/0}$, and smaller in films made with PEG-400 compared to PEG-1000.

The presence of PEG-1000 in PUA as the soft segment leads to fewer intermolecular hydrogen bonds forming between the hard segments, resulting in a reduced T_g of the films [18, 21]. The broad endothermic peak observed at 140 °C in $PUA_{4\text{-}2/0}$ may be related to the melting of the soft segment crystalline region.

TGA Studies

Table 4 displays the results of the thermal stability test of PUAs in a nitrogen atmosphere. The initial mass loss of 1–5% at 124–249 °C is due to the desorption of volatile content. The urethane bond in PUAs is known to be thermally unstable and starts to decompose at around 250–320 °C [7]. This indicates that degradation begins with the urethane bond, followed by the ester bond in the soft segment [22]. Figure 6 illustrates the three-step degradation process observed in the DTG curves of PUAs. The first stage is characterized by the decomposition of the hard segments from the urethane linkages, resulting in the formation of isocyanates and alcohols [22–25]. The second stage is caused by the degradation of the soft segments [22]. Finally, the

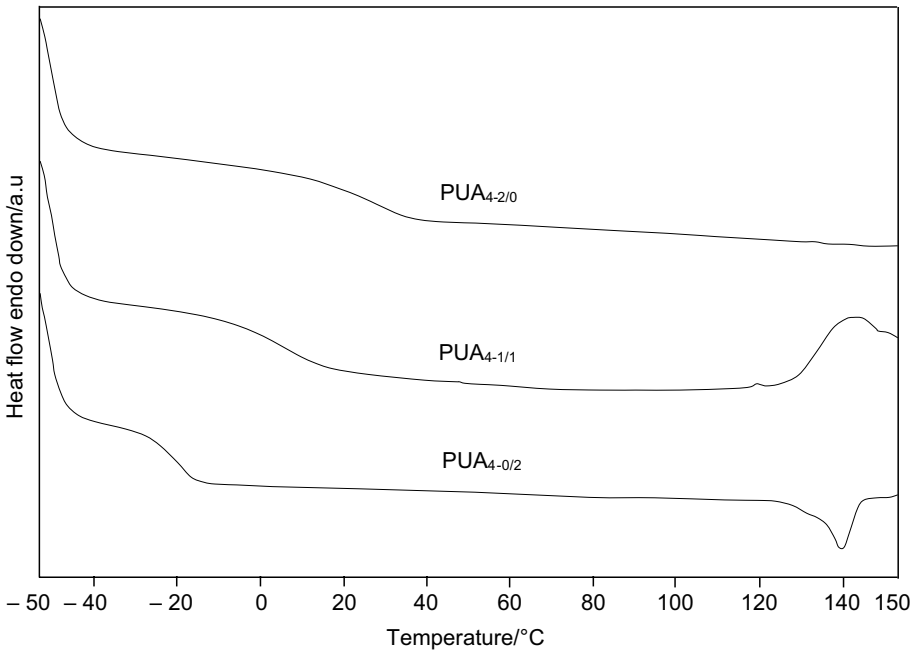

Fig. 4 DSC curves of different PUA samples having PEG-400

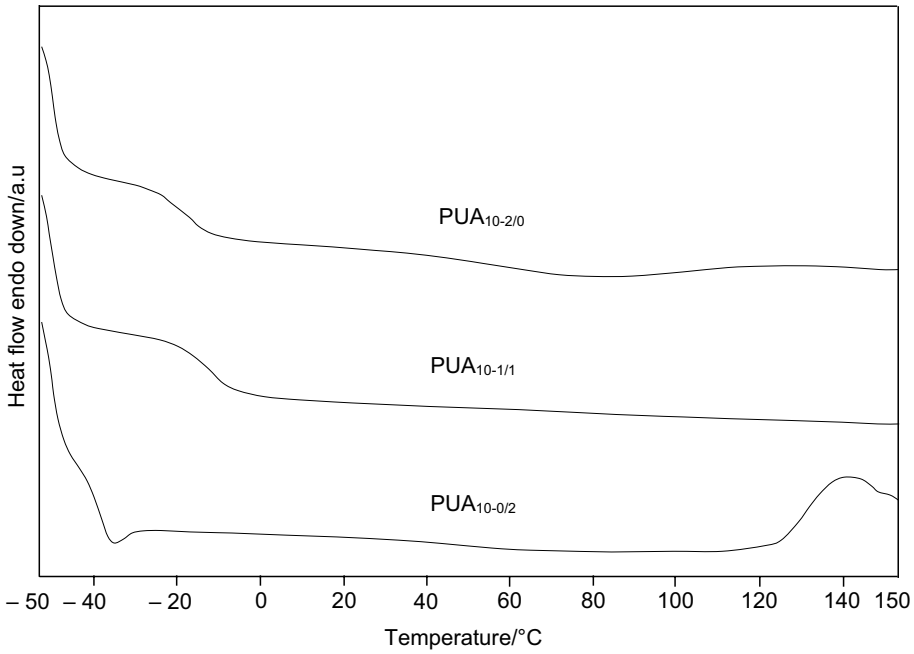

Fig. 5 DSC curves of different PUA samples having PEG-1000

Table 3 DSC data of PUA samples

Sample	T_g /°C	ΔC_p /J g^{-1} °C^{-1}
$PUA_{4\text{-}2/0}$	26.26	0.367
$PUA_{4\text{-}1/1}$	5.55	0.415
$PUA_{4\text{-}0/2}$	− 18.76	0.269
$PUA_{10\text{-}2/0}$	− 32.6	0.176
$PUA_{10\text{-}1/1}$	− 26.28	0.217
$PUA_{10\text{-}0/2}$	− 38.03	0.749

third stage is characterized by the decomposition of hydrocarbon chains. The following data were determined from DTG curves: (a) $T_{5\%}$, $T_{10\%}$, $T_{30\%}$, and $T_{50\%}$, the temperature at which 5,10, 30, and 50 mass % degradations occurred, respectively. (b) $T_{max1,}$ $T_{max2,}$ and T_{max3} are the temperatures at the first, the second and the third maximum mass loss rate in the DTG.

The PUA samples with PEG-400 have lower thermal stability compared to those with PEG-1000. As an example, the degradation temperature (T_d) of the $PUA_{4\text{-}0/2}$ film at 5%, 10%, 30%, and 50% mass losses was 124, 193, 280, and 309 °C, respectively. Meanwhile, the T_d of the $PUA_{10\text{-}0/2}$ film at 5%, 10%, 30%, and 50% mass losses was 233, 263, 332, and 375 °C, respectively. Microphase separation increases the thermal stability of PUAs by dissociating intermolecular hydrogen bonding between urethane groups at higher degradation temperatures. The increased thermal stability in PUAs with higher microphase separation is due to fewer residual hard segments. The lower T_{max2} value of $PUA_{4\text{-}2/0}$ compared to $PUA_{4\text{-}0/2}$ indicates that the hydrogen bonds between the urethane segments of $PUA_{4\text{-}0/2}$ dissociate at higher temperatures during degradation than those of $PUA_{4\text{-}2/0}$. This suggests that the hydrogen bonds in $PUA_{4\text{-}0/2}$ are stronger or more stable, leading to a lower dissociation temperature compared to $PUA_{4\text{-}2/0}$.

The shoulder observed in the temperature range of 420–470 °C with a maximum at 430 °C in PUA with PEG-400 films is a result of the degradation of acrylic polyol component. The T_{max2} at around 300 °C is related to the thermal degradation of the hard segments from the urethane linkages. The new degradation step at around 430 °C is specifically attributed to the degradation of acrylic polyol. This shoulder was only seen in PUA samples that contained acrylic polyol, indicating that it is unique to this component.

The results showed that the third degradation step of $PUA_{4\text{-}2/0}$ and $PUA_{10\text{-}2/0}$ corresponded to the gradual degradation of the char residue. The T_{max3} of $PUA_{4\text{-}2/0}$ was higher than that of $PUA_{10\text{-}2/0}$, indicating that the molecular mass of the PEG influenced the thermal stability of the PUA films. The temperature range for the third step of $PUA_{4\text{-}2/0}$ was from 509 to 727 °C, with a T_{max3} at 686 °C and a mass loss of 29.78%. For the $PUA_{10\text{-}2/0}$ sample, the third step was found in the temperature range of 485 to 650 °C, with a T_{max3} of 600 °C.

Table 4 shows that as the length of the soft segment increases, the maximum thermal degradation rate in the second degradation step also increases. The maximum degradation rate increases from 7.76% min^{-1} for $PUA_{4\text{–}2/0}$ to 13.64% min^{-1} for $PUA_{10\text{-}2/0}$. The maximum rate of degradation in the third decomposition step decreases as the length of the soft segment increases. The $PUA_{10\text{-}2/0}$ sample

Table 4 The thermal properties of PUA samples

Sample	Thermal degradation step	T_{max}/°C	$(dw/dt)_{max}$ /% min^{-1}	$T_{5\%}$/°C	$T_{10\%}$/°C	$T_{30\%}$/°C	$T_{50\%}$/°C
$PUA_{4\text{-}2/0}$	I	270	1.28				
	II	330	7.76	248	273	316	345
	III	686	0.64				
$PUA_{4\text{-}1/1}$	I	270	0.83				
	II	332,430sh	8.11	154	235	306	334
	III	659	0.79				
$PUA_{4\text{-}0/2}$	I	270	0.78				
	II	337, 430sh	9.50	124	193	280	309
	III	637	0.51				
$PUA_{10\text{-}2/0}$	I	330	4.52				
	II	389	13.64	249	282	344	375
	III	600	0.53				
$PUA_{10\text{-}1/1}$	I	330	4.21				
	II	393	12.67	240	276	332	386
	III	603	0.45				
$PUA_{10\text{-}0/2}$	I	300	2.34				
	II	399	14.27	233	263	332	375
	III	612	0.47				

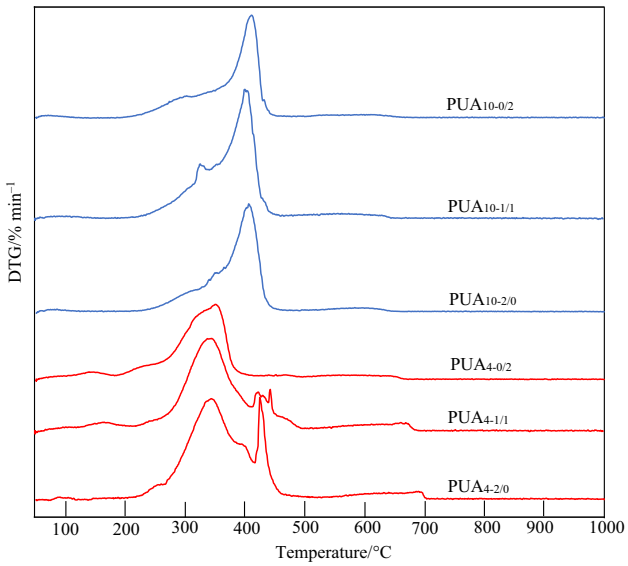

Fig. 6 DTG curves of PUAs

showed a lower maximum thermal degradation rate compared to the $PUA_{4\text{-}2/0}$ sample (0.64 and 0.53% min^{-1} for $PUA_{4\text{-}2/0}$ and $PUA_{10\text{-}2/0}$, respectively). In the second degradation step, the PUA with PEG-400 samples showed the lower thermal stability compared to the PUA with PEG-1000 samples, while in the last step of degradation it was reversed. The reason behind this observation is not clear and requires further investigation.

Table 5 Gloss and contact angle measurements of PUA films

Sample	Gloss /°			Contact Angle /°
	20	60	85	
$PUA_{4\text{-}2/0}$	160	151	106	72
$PUA_{4\text{-}1/1}$	174	160	101	64
$PUA_{4\text{-}0/2}$	131	140	105	45
$PUA_{10\text{-}2/0}$	79	124	90	50
$PUA_{10\text{-}1/1}$	111	126	97	45
$PUA_{10\text{-}0/2}$	80	121	95	30

Film properties of PUAs

Gloss of PUA films was measured at an angle of 20°, 60°, and 85° (Table 5). The gloss decreases with increasing HEMA content owing to the low refractive index of HEMA. The gloss values obtained at an angle of 60° are 160 and 140 for $PUA_{4\text{-}1/1}$ and $PUA_{4\text{-}0/2}$ films, respectively. This indicates that the PUA film with a higher HEMA content ($PUA_{4\text{-}0/2}$) has lower gloss compared to the PUA film with lower HEMA content ($PUA_{4\text{-}1/1}$) at an angle of 60 degrees. The low refractive index of HEMA causes light to scatter in many directions, hence reducing the gloss.

The gloss of PUA with PEG-1000 is lower than those of the corresponding PUA with PEG-400. This reduction in gloss is due to the formation of micro roughness domains caused by PEG-1000, which results in a decrease in the smoothness of the surface and a lower gloss value. The presence of microphase separation and surface roughness in PUA films

containing PEG-1000 leads to a decrease in overall gloss compared to those containing PEG-400 [26, 27].

The contact angle (CA) measures the wettability of a material, and a high CA value means that the material is highly hydrophobic, while a low CA value means that the material is highly hydrophilic. In the case of $PUA_{4\text{-}1/1}$, the CA value of 64° indicates higher hydrophobicity compared to $PUA_{10\text{-}1/1}$ with a CA value of 45°, which shows lower hydrophobicity. This result shows that the PUA film with PEG-1000 has a higher hydrophilicity compared to the PUA film with PEG-400, which is mainly attributed to the microphase separation behavior of the PUAs. The difference in hydrogen bonding force in the hard segments leads to the difference in hydrophobicity/hydrophilicity of the surface [28–30]. The results from gloss and contact angle tests are in agreement with those obtained from FTIR, DSC and TGA studies. This correlation between HEMA content and hydrophilicity can be attributed to the presence of hydrophilic functional groups (OH) in HEMA, which increases the surface energy of the PUA films and make them more hydrophilic. The hydrophobic functional groups in the other components of the PUA films, on the other hand, decrease the surface energy and make the films more hydrophobic. The balance between these two types of functional groups determines the overall hydrophilicity/hydrophobicity of the films.

Morphological study of PUAs

The SEM images indicated that the surface morphology and phase behavior of PUAs were influenced by the length of PEG. The microphase separation caused by PEG led to the formation of irregular spots and wrinkles in PUA with PEG-400, while the addition of PEG-1000 resulted in cracks on the surface of the PUA film (Fig. 7). With an increase in the content of

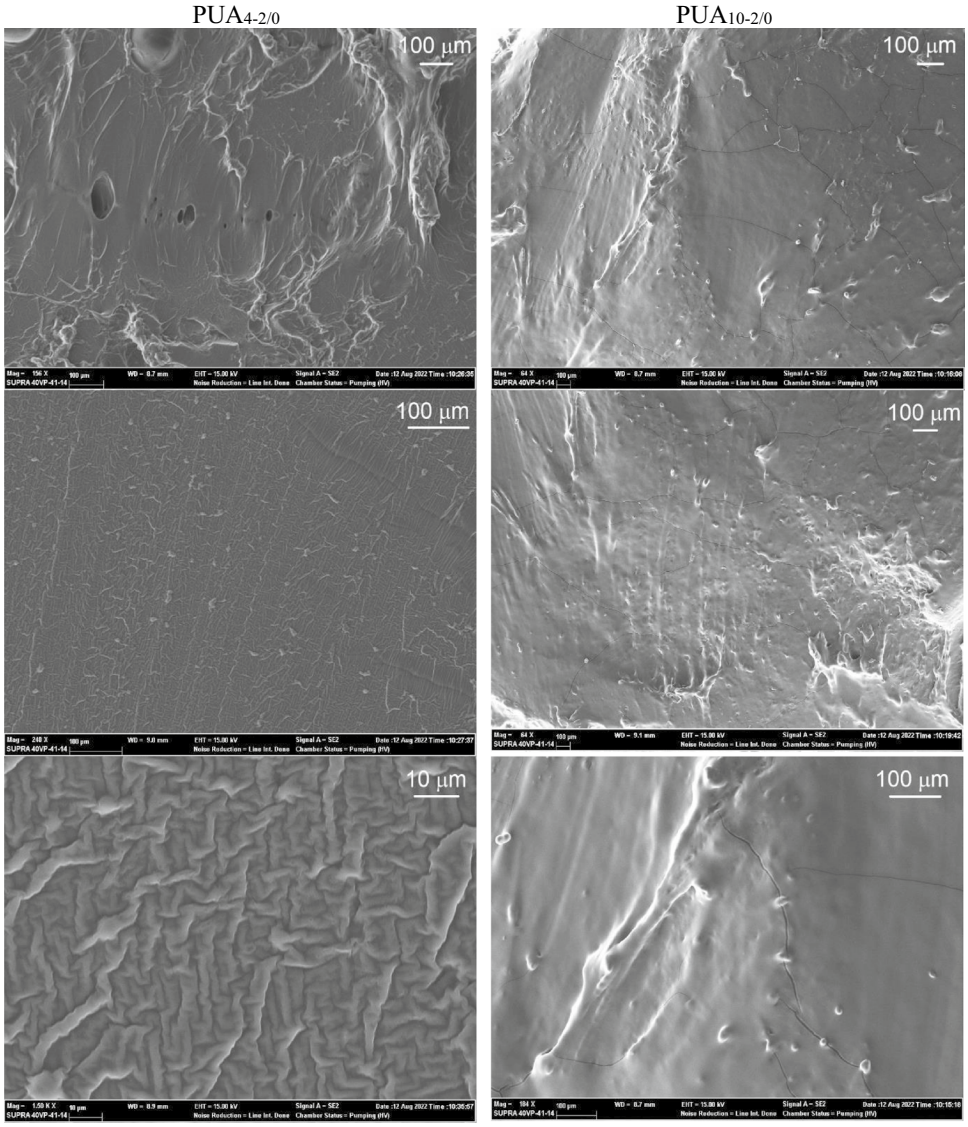

Fig. 7 The representative SEM images of PUA films

hard segments and intensification of the reaction, the cracks in $PUA_{10\text{-}2/0}$ expanded, leading to the formation of holes that were noticeably evident. On the other hand, in $PUA_{4\text{-}2/0}$, the irregular and non-spherical sporadic spots were a result of poor compatibility between hard and soft segments. This incompatibility also contributed to chemical composition inhomogeneity in the PUA and led to the percolation of hard segments from soft segments, indicating good microphase separation. These findings agreed with the results from other characterization techniques, such as FTIR, DSC, TGA, and gloss and contact angle measurements, and indicated that the length of PEG played an important role in the physical properties of PUA films.

Conclusions

This study aimed to examine how different molecular masses of PEG and HEMA affect the properties of PUA films, including their thermal, morphological, and hydrophilic/hydrophobic properties. The findings, which were based on a range of analyses such as DSC, FTIR, TGA/DTG, SEM, gloss, and water contact angle, indicated that microphase separation morphology is dominant in PUA films with PEG-1000, and that this has a significant impact on their hydrophilicity. The results suggest that these findings could be used to develop new PUA materials with improved properties. The size of microphase separation in PUAs using PEG-400 and PEG-1000 varies depending on their molecular mass and compatibility with hard segments. PEG-1000 has a higher molecular mass, making it more compatible with hard segments and resulting in a larger size of microphase separation that forms hydrogen bonding between urethane NH and carbonyls. PEG-400, with its smaller molecular mass, results in a smaller size of microphase separation. The degree of phase mixing in PUA with PEG-400 is higher, leading to an increase in T_g compared to PUA with PEG-1000. This increased degree of phase mixing is due to the increased hard domains resulting from the compatibility between hard segments and PEG-400, as they have similar polarity. This leads to a more homogeneous distribution of hard and soft domains in PUA with PEG-400 compared to PUA with PEG-1000. The thermal degradation behaviors of PUA films were analyzed using TG/DTG, with the first degradation step at 270–330 °C related to the degradation of urethane groups in hard segments, the second degradation step at 330 °C attributed to the degradation of soft segments, and the degradation at 430 °C associated with the degradation of acrylic polyol. The last stage, observed above 600 °C, shows gradual degradation of char residue. PUA with PEG-400 showed less thermal stability than PUA with PEG-1000 in the second degradation step, while in the third step, this was reversed. The length of the soft segment affects the maximum thermal degradation rate, with an increase in the length of PEG content resulting in an increase in the maximum thermal degradation rate during the second degradation step, but a decrease during the third decomposition step. The reason for this discrepancy requires further investigation.

Supplementary Information The online version contains supplementary material available at https://doi.org/10.1007/s10973-023-12507-4.

Acknowledgements This study was supported by Bilecik Şeyh Edebali University with the project number 2018-01.BŞEÜ.04-07. The authors also thank DYO Paint Factories, Izmir, for the polymers' DSC analysis, contact angle, and gloss measurements.

Author contributions BE is responsible for processing the experimental data, conducting the analysis, and creating the figures. EDK is responsible for performing the experiments. BE is responsible for performing the polymer characterization. EE is responsible for writing the draft of the manuscript.

References

1. Rao Z, Yan H, Tao W, Liu C, Jian G, Zhou Y, Chen H, Yang M. Effects of aminopropyl-terminated polydimethylsiloxane on structure and properties of waterborne polyurethane-acrylate. Prog Org Coat. 2023;174:107314. https://doi.org/10.1016/j.porgcoat.2022.107314.
2. Choi J-S, Seo J, Khan SB, Jang ES, Han H. Effect of acrylic acid on the physical properties of UV-cured poly(urethane acrylate-co-acrylic acid) films for metal coating. Prog Org Coat. 2011;71:110–6. https://doi.org/10.1016/j.porgcoat.2011.01.005.
3. Dong F, Qian Y, Xu X, Shaghaleh H, Guo L, Liu H, Wang S. Preparation and characterization of UV-curable waterborne polyurethane using isobornyl acrylate modified via copolymerization. Polym Degrad Stab. 2021;184:109474. https://doi.org/10.1016/j.polymdegradstab.2020.109474.
4. Khasraghia SS, Shojaeia A, Sundararaj U. Bio-based UV curable polyurethane acrylate: morphology and shape memory behaviors. Eur Polym J. 2019;118:514–27. https://doi.org/10.1016/j.eurpolymj.2019.06.019.
5. Choia J-S, Seob J, Khanc SB, Janga ES, Han H. Effect of acrylic acid on the physical properties of UV-cured poly(urethane acrylate-co-acrylic acid) films for metal coating. Prog Org Coat. 2011;71:110–6. https://doi.org/10.1016/j.porgcoat.2011.01.005.
6. Sanai Y, Ninomiya T, Arimitsu K. Improvements in the physical properties of UV-curable coating by utilizing type II photoinitiator. Prog Org Coat. 2021;151:106038. https://doi.org/10.1016/j.porgcoat.2020.106038.
7. Wang X, Soucek MD. Investigation of non-isocyanate urethane dimethacrylate reactive diluents for UV-curable polyurethane coatings. Prog Org Coat. 2013;76:1057–67. https://doi.org/10.1016/j.porgcoat.2013.03.001.
8. Fu J, Yu H, Wang L, Fahad S. Preparation and properties of UV-curable diamine-based polyurethane acrylate hard coatings. Appl Surf Sci. 2020;533:147442. https://doi.org/10.1016/j.apsusc.2020.147442.
9. Xu H, Qiu F, Wang Y, Wu W, Yang D, Guo Q. UV-curable waterborne polyurethane-acrylate: preparation, characterization

and properties. Prog Org Coat. 2012;73:47–53. https://doi.org/10.1016/j.porgcoat.2011.08.019.
10. Peruzzoa PJ, Anbindera PS, Pardinia OR, Vegac J, Costad CA, Galembeckd F, Amalvy JI. Waterborne polyurethane/acrylate: Comparison of hybrid and blend systems. Prog Org Coat. 2011;72:429–37. https://doi.org/10.1016/j.porgcoat.2011.05.016.
11. Fu J, Yu H, Wang L, Lin L, Khan RU. Preparation and properties of UV-curable hyperbranched polyurethane acrylate hard coatings. Prog Org Coat. 2020;144:105635. https://doi.org/10.1016/j.porgcoat.2020.105635.
12. Keramatinia M, Najafi F, Saeb MR. Synthesis and viscoelastic properties of acrylated hyperbranched polyamidoamine UV-curable coatings with variable microstructures. Prog Org Coat. 2017;113:151–9. https://doi.org/10.1016/j.porgcoat.2017.09.005.
13. Kunwong D, Sumanochitraporn N, Kaewpirom S. Curing behavior of a UV-curable coating based on urethane acrylate oligomer: the influence of reactive monomers, Songklanakarin. J Sci Technol. 2011;33:201–7.
14. Yildiz Z, Onen HA, Gungor A, Wang Y, Jacob K. Effects of NCO/OH ratio and reactive diluent type on the adhesion strength of polyurethane methacrylates for cord/rubber composites. Polym Plast Technol Eng. 2018;57:935–44. https://doi.org/10.1080/03602559.2017.1364382.
15. Gite VV, Mahulikar PP, Hundiwale DG. Preparation and properties of polyurethane coatings based on acrylic polyols and trimer of isophorone diisocyanate. Prog Org Coat. 2010;68:307–12. https://doi.org/10.1016/j.porgcoat.2010.03.008.
16. Cheng B-X, Gao W-C, Ren X-M, Ouyang X-Y, Zhao Y, Zhao H, Wu W, Huang C-X, Liu Y, Liu X-Y, Li H-N, Li RKY. A review of microphase separation of polyurethane: Characterization and applications. Polym Test. 2022;107:107489. https://doi.org/10.1016/j.polymertesting.2022.107489.
17. Fakhar A, Sadeghi M, Dinari M, Lammertink R. Association of hard segments in gas separation through polyurethane membranes with aromatic bulky chain extenders. J Membr Sci. 2019;574:136–46. https://doi.org/10.1016/j.memsci.2018.12.062.
18. Choperena A, Painter P. Hydrogen bonding in polymers: effect of temperature on the OH stretching bands of poly(vinylphenol). Macromolecules. 2009;42:6159–65. https://doi.org/10.1021/ma900928z.
19. Sultan M, Atta S, Bhatti HN, Islam A, Jamil T, Bibi I, Gull N. Synthesis, characterization, and application studies of polyurethane acrylate thermoset coatings: effect of hard segment. Polym Plast Technol Eng. 2017;56:1608–18. https://doi.org/10.1080/03602559.2017.1280736.
20. Zubera M, Shaha SAA, Jamil T, Asghar MI. Performance behavior of modified cellulosic fabrics using polyurethane acrylate copolymer. Int J Biol Macromol. 2014;67:254–9. https://doi.org/10.1016/j.ijbiomac.2014.03.021.
21. Huang H, Pang H, Huang J, Yu P, Li J, Lu M, Liao B. Influence of hard segment content and soft segment length on the microphase structure and mechanical performance of polyurethane-based polymer concrete. Constr Build Mater. 2021;284:122388. https://doi.org/10.1016/j.conbuildmat.2021.122388.
22. Paraskar PM, Hatkar VM, Kulkarni RD. Facile synthesis and characterization of renewable dimer acid-based urethane acrylate oligomer and its utilization in UV-curable coatings. Prog Org Coat. 2020;149:105946. https://doi.org/10.1016/j.porgcoat.2020.105946.
23. Molavi H, Shojaei A, Mousavi SA. Photo-curable acrylate polyurethane as efficient composite membrane for CO2 separation. Polymer. 2018;149:178–91.
24. Xiang H, Wang X, Xi L, Dong H, Hong P, Su J, Cui Y, Liu X. Effect of soft chain length and generation number on properties of flexible hyperbranched polyurethane acrylate and its UV-cured film. Prog Org Coat. 2018;114:216–22. https://doi.org/10.1016/j.porgcoat.2017.10.019.
25. Wang T-L, Hsieh T-H. Effect of polyol structure and molecular weight on the thermal stability of segmented poly(urethaneureas). Polym Degrad Stab. 1997;55:95–102. https://doi.org/10.1016/S0141-3910(96)00130-9.
26. Fakhar A, Sadeghi M, Dinari M, Mo. Zarabadipoor, R. Lammertink,. Elucidating the effect of chain extenders substituted by aliphatic side chains on morphology and gas separation of polyurethanes. Eur Polym J. 2020;122:109346. https://doi.org/10.1016/j.eurpolymj.2019.109346.
27. Xie T, Kao W, Zhang Z, Liu Y, Li Z. Synthesis and characterization of organosilicon modified self-matting acrylate polymer: ınsight into surface roughness and microphase separation behavior. Prog Org Coat. 2021;157:106300. https://doi.org/10.1016/j.porgcoat.2021.106300.
28. Khasraghia SS, Shojaei A, Sundararaj U. Bio-based UV curable polyurethane acrylate: morphology and shape memory behaviors Eur. Polym J. 2019;118:514–27. https://doi.org/10.1016/j.eurpolymj.2019.06.019.
29. Bari SS, Mishra S. Effect of calcium sulphate nanorods on mechanical properties of chitosan-hydroxyethyl methacrylate (HEMA) copolymer nanocomposites. Carbohydr Polym. 2017;157:409–18. https://doi.org/10.1016/j.carbpol.2016.09.083.
30. Lin YH, Liao KH, Chou NK, Wang SS, Chu SH, Hsieh KH. UV-curable low-surface-energy fluorinated poly(urethane-acrylate) s for biomedical applications. Eur Polym J. 2008;44:2927–37. https://doi.org/10.1016/j.eurpolymj.2008.06.030.